SANDIA REPORT
SAND2000-2927
Unlimited Release
Printed November 2000

LDRD Final Report: Raman Spectroscopic Measurements to Monitor the HMX β-δ Phase Transition

Alexander S. Tappan, Anita M. Renlund, and Jill C. Miller

Prepared by
Sandia National Laboratories
Albuquerque, New Mexico 87185 and Livermore, California 94550

**Sandia is a multiprogram laboratory operated by Sandia Corporation,
a Lockheed Martin Company, for the United States Department of Energy under Contract DE-AC04-94AL85000.**

Issued by Sandia National Laboratories, operated for the United States Department of Energy by Sandia Corporation.

Available to DOE and DOE contractors from
U.S. Department of Energy
Office of Scientific and Technical Information
P.O. Box 62
Oak Ridge, TN 37831

Telephone: (865)576-8401
Facsimile: (865)576-5728
E-Mail: reports@adonis.osti.gov
Online ordering: http://www.doe.gov/bridge

Available to the public from
U.S. Department of Commerce
National Technical Information Service
5285 Port Royal Rd
Springfield, VA 22161

Telephone: (800)553-6847
Facsimile: (703)605-6900
E-Mail: orders@ntis.fedworld.gov
Online order: http://www.ntis.gov/ordering.htm

SAND2000-2927
Unlimited Release
Printed November 2000

LDRD Final Report: Raman Spectroscopic Measurements to Monitor the HMX β-δ Phase Transition

Alexander S. Tappan, Anita M. Renlund and Jill C. Miller
Explosive Projects & Diagnostics Department
Sandia National Laboratories
P.O. Box 5800
Albuquerque, NM, 87185-1454

ABSTRACT

The HMX β-δ solid-solid phase transition, which occurs as HMX is heated near 170 °C, is linked to increased reactivity and sensitivity to initiation. Thermally damaged energetic materials (EMs) containing HMX therefore may present a safety concern. Information about the phase transition is vital to predictive safety models for HMX and HMX-containing EMs. We report work on monitoring the phase transition with real-time Raman spectroscopy aimed towards obtaining a better understanding of physical properties of HMX through the phase transition. HMX samples were confined in a cell of minimal free volume in a displacement-controlled or load-controlled arrangement. The cell was heated and then cooled at controlled rates while real-time Raman spectroscopic measurements were performed. Raman spectroscopy provides a clear distinction between the phases of HMX because the vibrational transitions of the molecule change with conformational changes associated with the phase transition. Temperature of phase transition versus load data are presented for both the heating and cooling cycles in the load-controlled apparatus, and general trends are discussed. A weak dependence of the temperature of phase transition on load was discovered during the heating cycle, with higher loads causing the phase transition to occur at a higher temperature. This was especially true in the temperature of completion of phase transition data as opposed to the temperature of onset of phase transition data. A stronger dependence on load was observed in the cooling cycle, with higher loads causing the reverse phase transitions to occur at a higher cooling temperature. Also, higher loads tended to cause the phase transition to occur over a longer period of time in the heating cycle and over a shorter period of time in the cooling cycle. All three of the pure HMX phases (α, β and δ) were detected on cooling of the heated samples, either in pure form or as a mixture.

ACKNOWLEDGEMENTS

The authors wish to acknowledge the contribution of Robert G. Schmitt (9116) for his ongoing contribution to the hot cell work. The authors also thank Kevin J. Fleming (2554) for the use of the Nd:YAG laser.

CONTENTS

FIGURES

TABLES

PREFACE

The work discussed here deals with an apparatus which is referred to as the “hot cell”. This is very different from and not to be confused with the Hot Cell Facility of Technical Area V.

EXECUTIVE SUMMARY

This report summarizes the work of a three-year LDRD project, entitled "Molecular Characterization of Energetic Material Initiation," initially funded in FY98. These results have been used to further Sandia National Laboratories Hazard Analysis Program (funded by the Office of Munitions) through the DOE / DoD Memorandum of Understanding, under Technology Coordination Group for Energetic Materials (TCG-III). This work has been presented at the Joint Army Navy NASA Air Force Propulsion Systems Hazards Subcommittee meetings in 1999 and 2000.[1,2] Abstracts for these two works can be found in the appendix.

NOMECLATURE

CCD	charge-coupled device
cookoff	explosion due to abnormal heating
EM	energetic material
HMX	1,3,5,7-tetranitro-1,3,5,7-tetraazacyclooctane
LVDT	linear variable differential transformer
LX-11	80% HMX, 20% Viton®

LDRD Final Report: Raman Spectroscopic Measurements to Monitor the HMX β-δ Phase Transition

INTRODUCTION

Sandia National Laboratories has responsibility for a diverse mix of energetic materials (EMs) and components. Determining the microscale chemical and physical responses of EMs to abnormal thermal environments is fundamental to understanding the safety of these EMs in cookoff (explosion due to abnormal heating) scenarios. The high explosive HMX (1,3,5,7-tetranitro-1,3,5,7-tetraazacyclooctane, Figure 1) is an energetic material used in many applications, from actuators to main charge explosives. Additionally it is often used in propellant formulations. Pure HMX can exist as three different crystallographic polymorphs, designated α, β and δ. Another form, γ-HMX, exists, but is a hydrate and will not be dealt with in this work. Table 1 shows a compilation of measured and calculated densities and temperature stability ranges for the three pure polymorphs.[3,4] Of the three phases, β-HMX is the thermodynamically stable phase and δ- HMX forms upon heating of β-HMX. The α phase can form from heating of β-HMX or cooling of δ-HMX and has a temperature stability range in between β- and δ-HMX. Both α- and δ-HMX are more sensitive to initiation. It is also important to note that α- and δ-HMX have lower densities than β-HMX and therefore the phase transitions result in a volumetric change, which can be observed as both a volume change and a force change, if the sample is mechanically confined. δ-HMX is of particular concern, because it readily forms upon heating of β-HMX and is the most sensitive of the three pure phases. The HMX β-δ solid-solid phase transition occurs as HMX is heated to around 170 °C, the exact temperature varying with heating rate, particle size and pressure.[4-8] It is well established that δ-HMX is more sensitive to initiation.[4] Furthermore, the increased porosity that results from the thermal and mechanical damage of heating can lead to an EM that is particularly sensitive to initiation and that has combustion properties that differ greatly from the pristine material. Initiation, reactive wave growth, and ultimately deflagration or detonation depend on chemical and physical processes at the microscale. Understanding the rate of phase transition as functions of temperature, particle size, pellet density and confinement are critical to predicting cookoff response for components and systems. Predictive models of EMs approaching cookoff conditions must incorporate both chemical

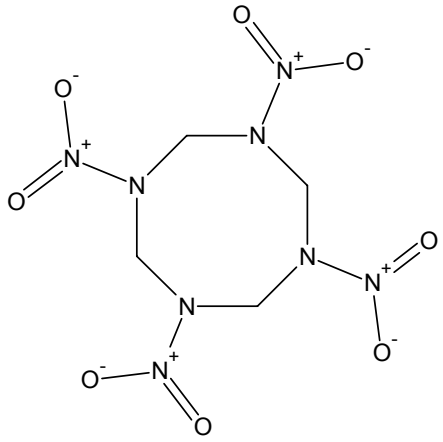

Figure 1. HMX (1,3,5,7-tetranitro-1,3,5,7-tetraazacyclooctane).

Table 1. HMX densities and temperature ranges for the three pure polymorphs. Compiled from references 3 and 4.

Form	Density (m)	Density (c)	Temperature Range (°C)
α	1.84	1.839	146-150 to 156-158.5
	1.83	1.848	115 to 156
		1.823	105 to 155
			102-104.5 to 160-164
β	1.9	1.894	r.t to 146-150
	1.91	1.943	r.t to 115
			r.t to 105
			r.t to 102-104.5
δ	1.8	1.786	156-158.5 to m.p.
		1.764	156 to m.p.
			155 to m.p.
			160-164 to m.p.

and physical changes that occur in the material as it is heated. Raman spectroscopy is an excellent method of monitoring crystallographic changes as HMX proceeds through the phase transition. The conformational differences between α-, β-, and δ-HMX lead to distinctly different Raman spectra. Raman spectroscopy is non-destructive, can give real-time data distinguishing the phases and is well suited for non-invasive monitoring. We have developed an experimental apparatus called the hot cell, which is used to examine the physical and chemical phenomena associated with the thermal degradation of EMs. The work presented here deals with the incorporation of a Raman spectroscopic probe into the hot cell and its use to examine, in real-time, the phase transitions of HMX in temperature ranges and confinement pressures relevant to component and system cookoff environments.

EXPERIMENTAL

The basic hot cell apparatus has been described previously.[1,2,9,10] The Raman hot cell apparatus, as seen in Figure 2, is similar to other hot cells with modifications to accommodate the Raman probe. It consists of a 6.35-mm diameter x 3.18-mm length (1/4 in. x 1/8 in.) explosive pellet confined within a cylindrical stainless steel cell. The pellet is confined from opposing ends by Invar® (a low thermal coefficient of expansion steel) pistons and sealed within the cell with Viton® O-rings. Four thermocouples (Omega, Stamford, CT) inserted into the cell regulate and measure the temperature as the cell is heated at a controlled ramp by a programmable controller and band heater (both, Watlow Controls, Winona, MN). The lower piston is threaded into a load cell (Sensotec, Columbus, OH), which measures the mechanical response of the pellet as it is heated. Two variations of the experiment exist, the difference being that in one, the volume of the cell is maintained constant, (displacement-controlled) and in the other, the axial load exerted on the pellet is maintained constant, (load-controlled). Initial experiments were conducted in the displacement-controlled variation. The final experiments in this report are load-controlled. The load cell is mechanically coupled to a pneumatic cylinder (Bimba, Monee, IL). The pneumatic cylinder allows the sample to be preloaded and also buffers changes in load as the sample expands and contracts during heating, by absorbing these changes into a large volume of compressible gas. This results in a relatively constant load on the sample throughout the experiment. Nitrogen gas is used to actuate the pneumatic cylinder. Chilled water circulated through a cooling plate at the bottom of the apparatus isolates the heating to the cell and protects the load cell from temperature-induced errors. A LVDT (linear variable differential transformer, Lucas Control Systems Products, Hampton, VA) extensometer measures the pellet length as the pellet expands and contracts with heating and the HMX phase transition. The entire load train is contained within a rigid Invar® load frame. Laser light is delivered and Raman scattered light is collected through a machined aperture in the top piston. A 1-mm thick sapphire window sealed against the top piston with a Viton® O-ring allows light transmission to and from the EM sample, while maintaining confinement. The cell was designed to minimize free volume and allow minimal air to be trapped in the cell during assembly. During the experiment, the apparatus is sealed in a vacuum chamber at roughly 100 mTorr. Any venting of the cell due to O-ring failure is detected by a sharp pressure rise in the chamber vacuum. Thermocouple, load cell and LVDT data are recorded by means of a custom software program (B&B Technologies, Albuquerque, NM) written in LabView™ (National Instruments Corporation, Austin, TX). HMX pellets were pressed on site at Sandia National Laboratories to a density of 1.8 g/cm^3 from powder. LX-11 (80% HMX, 20% Viton®) samples were manufactured at Lawrence Livermore National Laboratory.

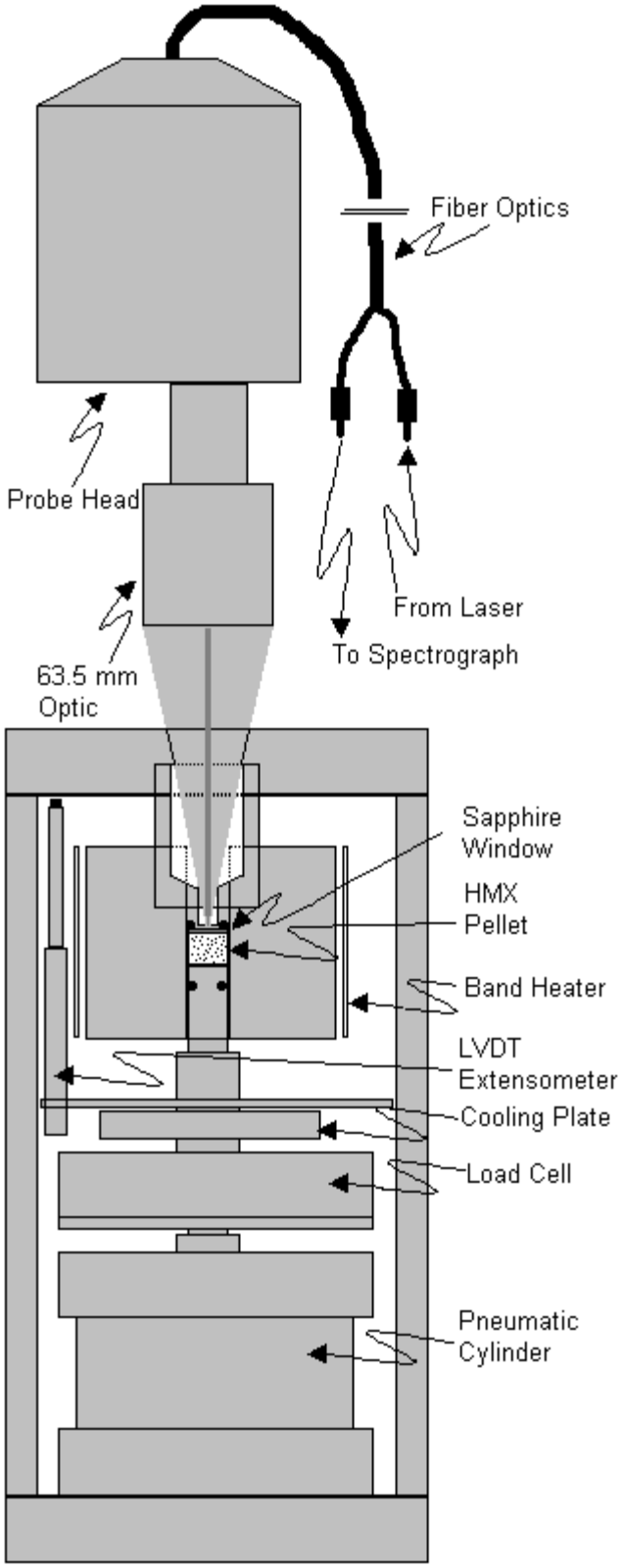

Figure 2. Raman hot cell apparatus.

The Raman signal is collected using a commercially available probe head (Kaiser Optical Systems, Inc., Ann Arbor, MI) with several modifications made for working in the evacuated environment of the explosives chamber. Laser light is launched into a 50-μm fiber optic, which delivers it to the body of the probe. On entering the probe, the light is filtered to remove the silica Raman and fluorescence, ensuring that only the pure laser light is delivered to the sample. 40–50 mW of 532-nm continuous-wave laser light is supplied by a frequency-doubled Nd:YAG (Adlas, Lübeck, Germany), and is focused to roughly a 100-μm diameter spot on the sample by a 63.5-mm working distance optic. The same optic collects and collimates the Raman scattered light from the EM sample, returning it to the body of the probe. A notch filter in the probe removes the laser line so that it does not generate silica Raman and fluorescence in the fiber that delivers the light to the spectrograph. A final optic launches the filtered light into this 100-μm fiber. This design removes much of the fluorescence by approximating a confocal arrangement, with the 100-μm fiber acting as the fluorescence-rejecting aperture. This pseudo-confocal optical arrangement discriminates against out-of-focus light and delivers to the spectrograph that light that contains only the highest ratio of Raman to fluorescence, maximizing the useful signal. The Raman probe is mounted in the explosives chamber above the hot cell with focusing accomplished by a z-translation stage. Light from the probe is delivered to a f/1.8 axial transmissive spectrograph (Kaiser Optical Systems, Inc., Ann Arbor, MI) equipped with a liquid nitrogen cooled charge-coupled-device (CCD) camera (Roper Scientific, Trenton, NJ). The spectral range of the spectrograph with the presently installed holographic transmission grating is –700 cm^{-1} to 1900 cm^{-1} relative to the laser excitation wavelength of 532 nm.

A brief note on the notation used throughout this paper is necessary. When possible, the three phase transitions (β-δ, δ-β and δ-α) will be referred to explicitly. Otherwise, the β-δ phase transition, which occurs during heating, will be referred to as the "forward" phase

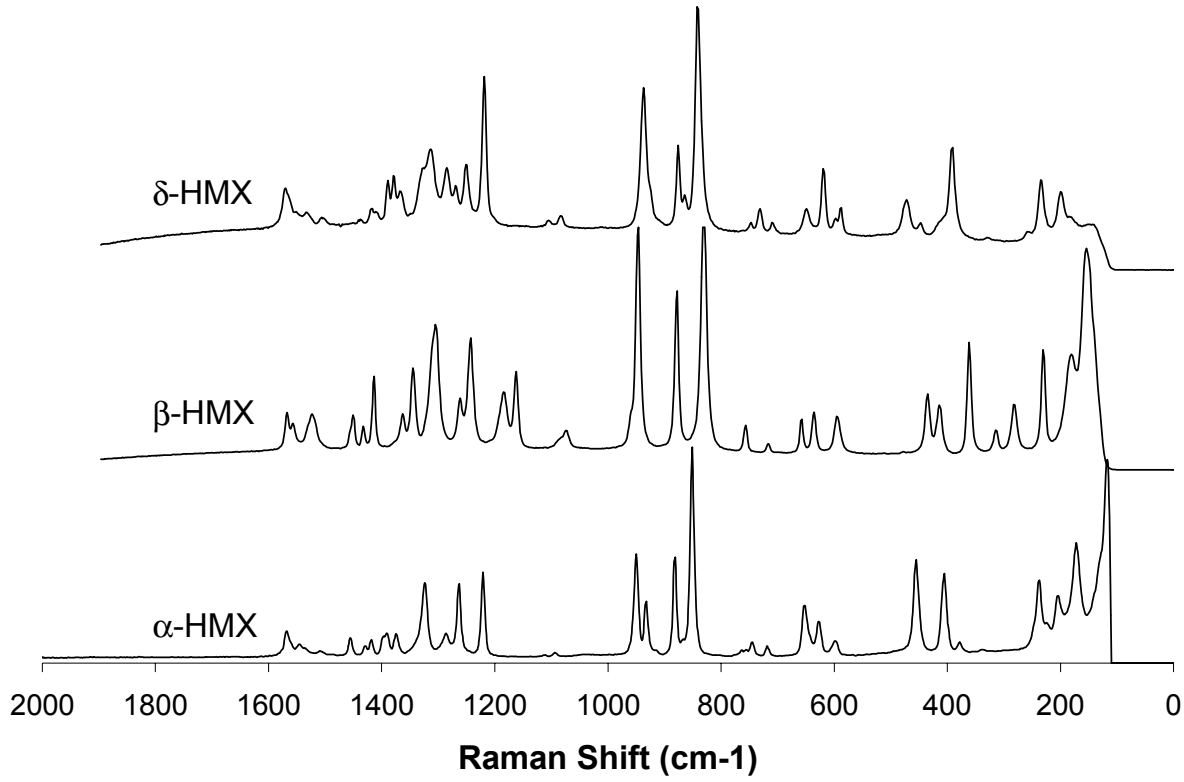

Figure 3. Raman spectra of α-, β-, and δ-HMX.

transition and the δ-β and δ-α phase transitions, which occur during cooling, will be referred to as the "reverse" phase transitions. It is important to note that the phase transitions can be incomplete and that mixtures of different phases can be present. Mixtures will be indicated by a slash between the two letters (e.g., α/β).

Identification of phase transitions

The criteria for observing the HMX phase transitions with Raman spectroscopy involve monitoring the presence or absence of peaks within two regions of the spectrum: the ring modes between 340 cm^{-1} and 460 cm^{-1} and the ring stretch modes between 800 cm^{-1} and 1000 cm^{-1}. These vibrational mode assignments were made separately by Iqbal et al. and Goetz and Brill.[5,11] The Raman spectra of α-, β-, and δ-HMX are shown in Figure 3. The β-HMX spectrum was obtained from a pure, pressed HMX pellet. The δ-HMX spectrum was obtained from a sample of δ-HMX, converted from β-HMX by heating. The α-HMX spectrum was provided by Bob Patton of Sandia National Laboratories, from a chemically recrystallized α-HMX sample. The forward, β-δ phase transition is identified by the disappearance of the peaks at 356 and 428 cm^{-1} and the appearance of the peak at 385 cm^{-1}. In addition, the peaks at 829 and 945 cm^{-1} disappear and are replaced by peaks at 841 and 932 cm^{-1}, respectively. The persistence of the peak at 412 cm^{-1} through the phase transition was consistent in all of the confined experiments. This result is inconsistent with results of Goetz and Brill.[5] The significance of this is not known. The reverse, δ-β phase transition is identified by observing the opposite of what was just described for the β-δ phase transition. The reverse, δ-α phase transition is identified by the disappearance

of the δ peaks at 387, and 936 cm^{-1} and the appearance of the α peaks at 398, 445, 829, 925 and 945 cm^{-1}. Based on the Raman data collected during several experiments, we confirmed that LVDT extensometer data and load data were valid indicators of the phase transitions. This is due to the fact that the different crystal phases have different densities, as listed in Table 1, and therefore, during a phase transition there is an expansion or contraction, which is observable in the LVDT extensometer and load cell data. LVDT extensometer data are presented as a comparison with Raman data in the "load-controlled experiments" section. The criteria for identifying the time of onset of a phase transition from the LVDT data involve estimating that point on the curve that is halfway through the acceleratory period, from a stable value, to a rapidly rising, or falling (if for one of the reverse phase transitions) value. The criteria for identifying the time of completion of a phase transtion from the LVDT data involve estimating that point on the curve that is halfway through the deceleratory period, from a rapidly rising, or falling (if for one of the reverse phase transitions) to a stable value. At several points in this work, reference to postmortem Raman analysis is made. This was always performed on the surfaces of the sample, as opposed to the interior. The kinetics are such that we have observed α- and δ-HMX to remain in samples for extended periods of time and thus, postmortem analysis can be used to confirm that a phase transition did occur.

RESULTS AND DISCUSSION

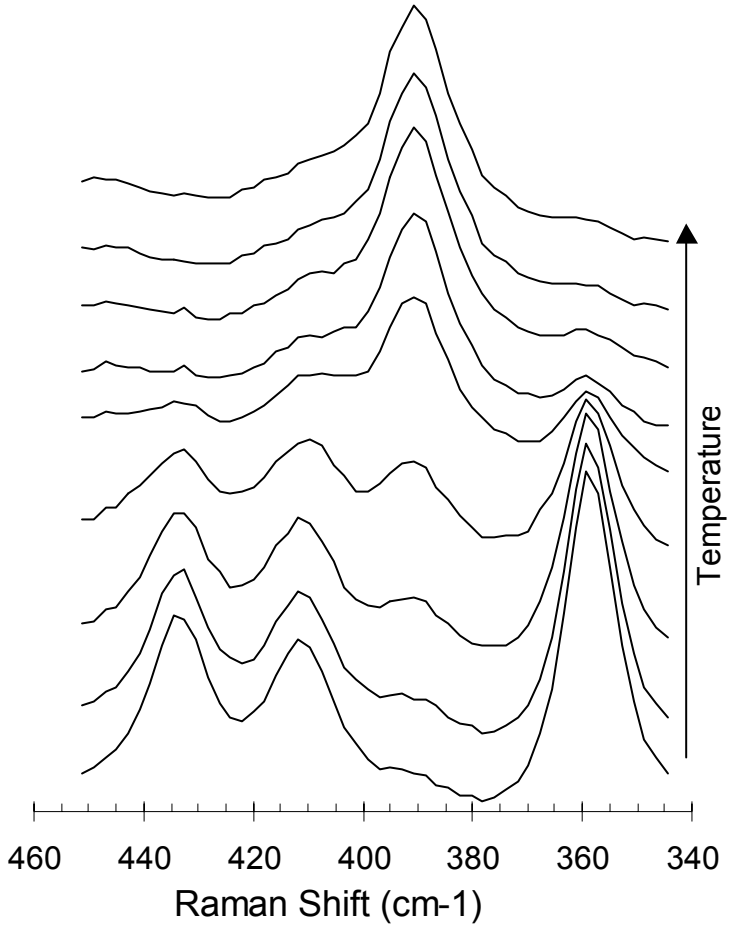

Figure 4. HMX β-δ phase transition in the unconfined experiment. Temperature range was approximately 170-180 °C.

Preliminary experiments

After selecting the above-mentioned spectrograph and Raman probe, the first experiment involved a simple feasibility study to determine if the β-δ phase transition was dynamically observable above the luminescence background (sample fluorescence, broadband thermal emission and silica Raman/fluorescence). A 6.35-mm diameter by 3.175-mm length 1.8-g/cm^3 pure HMX pellet was positioned in the cell, but was not confined and was open to atmosphere at one end. The Raman probe was positioned outside of the explosives chamber and light to and from the sample was delivered through a fused silica window mounted in the chamber. Laser light from the probe was focused onto the unconfined face of the pellet and spectra were collected every 30 seconds. CCD camera exposure time was 3 seconds. The pellet was heated to 140 °C at a rate of 7 K/minute, at which point the heating rate was reduced to 1

K/minute to ensure resolution of the expected spectral changes associated with the phase transition. Heating was continued at this rate until the completion of the phase transition was observed. Figure 4 shows the spectral changes that occurred during this experiment, in the region of 340 to 460 cm^{-1}, as the sample was heated through the β-δ phase transition. The figure consists of nine spectra, proceeding from bottom to top, as the cell was taken through the temperature range of approximately 170 to 180 °C. The temperature of the pellet face, sampled by the Raman probe, was not known exactly and therefore, no attempt was made to assign an exact temperature to each spectrum. The phase transition was clearly observed with this technique, as evidenced by the disappearance of the peaks at 360, 412 and 434 cm^{-1}, indicative of β-HMX and the growth of the peak at 391 cm^{-1}, indicative of δ-HMX.

After demonstrating that the phase transition was observable with available instruments, the probe was integrated into the test cell as shown in Figure 2 with the exception that the pneumatic cylinder was not used at this point and cooling water was applied to the top plate of the load frame, as well as to the lower plate. Experiments were first conducted on pressed 1.8-g/cm^3 HMX pellets to attempt to monitor the phase transition in this arrangement. Sample preloads ranged from 14 to 42 MPa (2000 to 6000 psi), with all but the first experiment conducted with the lower preloads. All samples experienced similar heating ramps: the cell was taken to 40 °C at a rate of 7 K /minute and held there for 30 minutes to allow for thermal equilibration, the cell was then taken to the final temperature of either 215 or 220 °C at a rate of 7 K /minute. The first series of experiments revealed that, although the bulk of the HMX sample underwent the phase transition, as evidenced by the load increase and postmortem Raman spectroscopy of the surfaces of the pellet, the area of the pellet sampled by the Raman probe was not undergoing a perceivable change. The volume expansion concomitant with the phase transition was being retarded by the cell confinement and only a certain percentage of the pellet was allowed to expand, that portion being that which first sees the heat from the band heater. As this portion of the pellet expanded, the remaining portion experienced higher pressures, could not expand and therefore was inhibited from undergoing the phase transition. The Raman probe sampled the top center of the pellet and because that portion of the pellet was in contact with sapphire, bounded by vacuum, rather than the steel and Invar® that the rest of the pellet was in contact with, it experienced the lowest temperatures. In later experiments, changes were made to increase the heat flux to the top of the pellet. The band heater was moved upwards on the cell, increasing the heat flux to the top of the cell and decreasing it to the bottom. The cooling water to the top plate was removed. Ceramic spacers were used to thermally isolate the top piston from the top plate, which could act as a heat sink. Preload of the pellet was decreased, providing lesser confinement. Experiments were conducted on pressed 1.7-g/cm^3 HMX pellets, because the lower density would allow more expansion, and a greater percentage of the pellet could undergo the phase transition. LX-11 (80% HMX, 20% Viton®) was examined, the reasoning being that the high percentage of compliant medium provided by the binder would allow more phase transition, accommodating expansion of individual HMX grains as the phase transition occurred. Broadband thermal emission was observed in all spectra, increasing as the EM was heated and thus indicating that the point of sampling was increasing in temperature, but none of these attempts allowed observation of the phase transition with Raman spectroscopy.

To determine if the above reasoning of cell confinement and HMX expansion inhibiting the phase transition was correct, two experiments were conducted in which a void was deliberately created at the top center of the pellet. The purpose of this void was to provide a volume into which that portion of the pellet could expand into, favoring the phase transition in that area. Circular aluminum foil disks were manufactured, 6.35-mm in diameter by 0.025-mm thick. A 1.65-mm diameter hole was cut in the center of the disks, providing a void space for a volume of the pellet to expand into, and also an orifice through which Raman could be sampled. In the first experiment five of these disks were placed on top of the

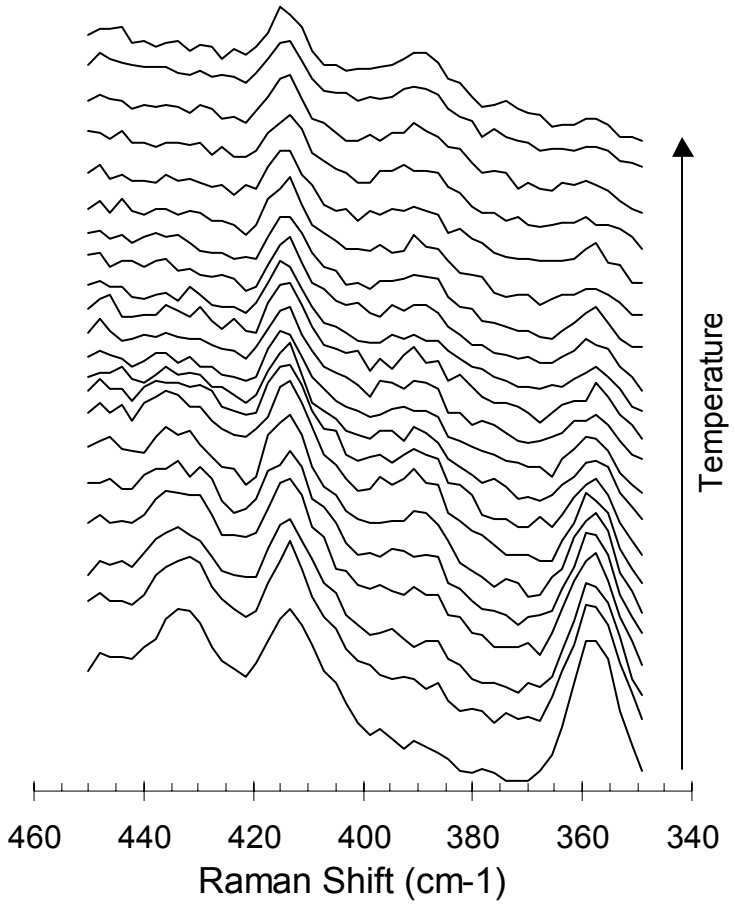

Figure 5. HMX β-δ phase transition in confined experiment with void. Temperature range was approximately 182-200 °C.

pellet, below the sapphire window, providing approximately 0.27 mm^3 of free volume into which the top portion of the pellet could expand. In the second experiment, four of these disks were used. HMX pellets, 6.35-mm diameter by 6.35-mm length and 1.7 g/cm^3 were used for both experiments. All of the previously mentioned steps to improve heat flux to the top portion of the pellet were taken. In the first of the two experiments, the phase transition was observed, but because the CCD camera saturated and the exposure time had to be changed during the experiment, the changes were not well resolved and the timing was inconsistent. Figure 5 shows the Raman data from the second test. Spectra were collected at 7.5-second intervals with six accumulated 0.5-second exposures comprising a three-second net exposure for each spectrum. The spectra shown were recorded in the cell temperature range of 182 °C to 200 °C, with the actual pellet temperature being lower, especially that portion of the pellet sampled by the Raman probe. The spectra were less well resolved than those in the unconfined experiment due to competing fluorescence from decomposition products. The phase transition was indicated by appearance of the peak at 390 cm^{-1} and disappearance of the peaks at 360 and 434 cm^{-1}. Note that the peak at 412 cm^{-1} persisted through the phase transition. This result is inconsistent with results of Goetz and Brill.[5] This was not observed in the unconfined experiment. The significance of this is not understood and it is not clear why only one and not all three of the peaks persisted. The spectral range of 800 cm^{-1} to 1000 cm^{-1}, although not shown in the figure, also confirms that the phase transition did occur. Figure 6 shows the temperature and load cell response in this experiment. The load response agreed with previous experiments.[1,2,9,10] As shown in the load cell response, thermal expansion of the material occurred to the point just before the phase transition at approximately 150 °C, where a shrinkage of the material occurred, shown by a decrease in the load. This shrinkage has been documented by Herrmann et al.[12] A sharp rise in the load was observed during the phase transition, in accordance with the lower density of the δ-phase. After the expansion of the phase transition completed, there was a drop in the load after which the load began to increase, due to pressure created by gaseous decomposition products. Indicated by the box on Figure 6 are the points in the temperature and the load history where the onset and end of the phase transition were indicated by Raman spectroscopy. These points correlate to the first and last spectra in Figure 5. The fact that the load began to increase before the phase transition was observed in the Raman spectrum agrees with heat flux being least to the top center of the pellet. The bulk of the pellet underwent the phase transition before the top center, which was the last part of the pellet to see the heat flux from the band heater. The fact that the phase transition completion was detected by the

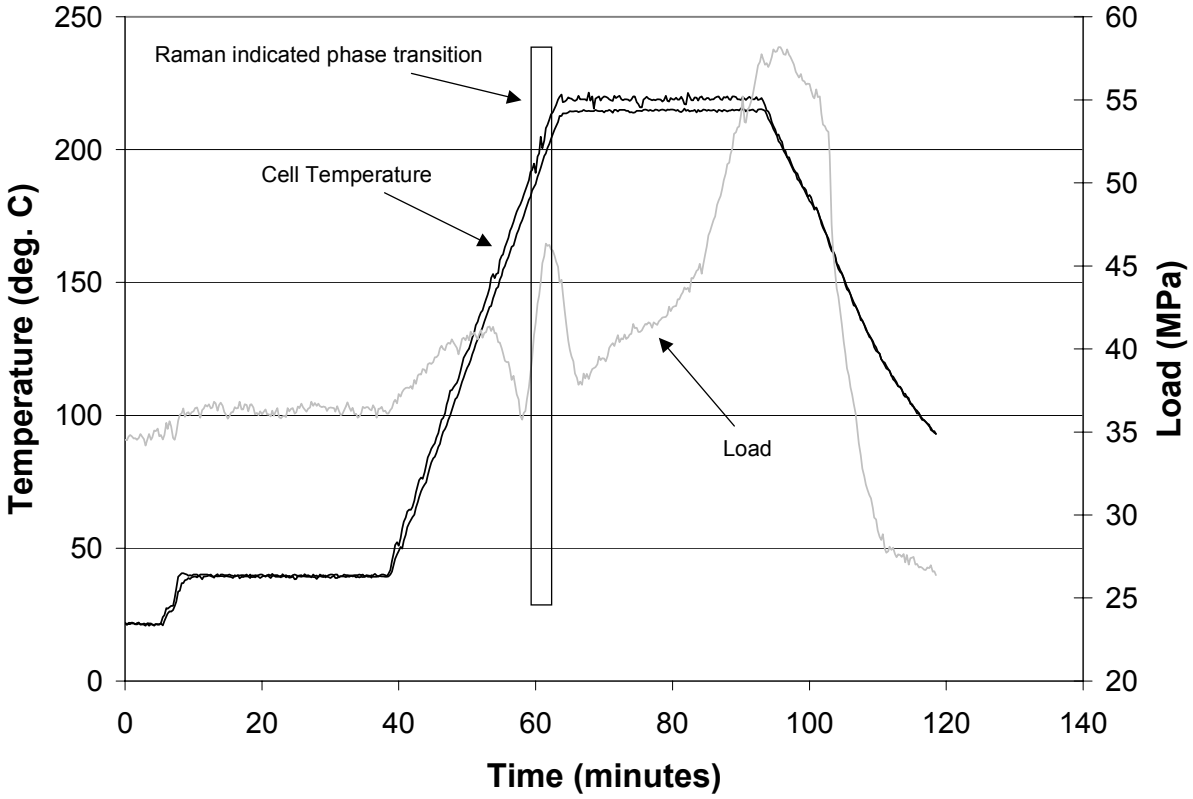

Figure 6. Temperature and load cell response for confined experiment with void. The box indicates the β-δ phase transition as detected by Raman spectroscopy.

load cell at the same time as detected by Raman spectroscopy indicates that this was indeed the last part of the pellet to phase transition. Postmortem visual inspection indicated that both samples did expand into the void provided by the foil disks, demonstrated by the samples retaining the shape of the expanded volume after cooling.

The implication of the experiments in the displacement-controlled apparatus is that at the higher loads reached, as the pellet begins to expand during the β-δ phase transition, the phase transition is retarded in other portions of the pellet due to the increasing pressure. This is due to the fact that increasing pressure inhibits the formation of δ-HMX due to its lower density as compared with β-HMX.[3] Due to the experiments in which the phase transition was indicated by the load cell response and also by postmortem Raman analysis, it was confirmed that not all areas of an HMX sample will necessarily undergo the phase transition. It was also confirmed that different phases could exist in the same sample. Based on these findings, it was decided to change from investigating the phase transition in the displacement-controlled hot cell to the load-controlled hot cell, which would allow lower loads to be maintained throughout an experiment. These results are discussed in the following section.

Load-Controlled Experiments

Based on the findings discussed in the previous section, the Raman hot cell was redesigned to accommodate the pneumatic cylinder as shown in Figure 2. This load-controlled hot cell allows a relatively constant load to be maintained throughout an experiment. The pneumatic cylinder accomplishes this by buffering expansion and contraction of the EM pellet into a relatively large volume of compressible gas. All of the experiments discussed in this section were conducted in the load-controlled Raman hot cell.

Upon completion of the load-controlled apparatus, experiments were conducted to determine if the HMX β-δ phase transition could be detected in this new configuration. Several experiments were conducted with the hot cell in the evacuated explosives chamber, as in the previous displacement-controlled experiments, taking the cell temperature above that at which the phase transition had been induced in other experiments. The phase transition was not detected by Raman spectroscopy in these experiments, even at lower loads, which should have allowed the phase transition to occur at lower temperatures. Based on these results, an experiment was conducted in which the sapphire window was not installed, exposing the surface of the sample directly to vacuum and therefore, Raman sampling occurred directly on the surface of the pellet. The results of this experiment are shown in Figure 7. The reasoning behind this experiment was that the sapphire window may have been confining the HMX sufficiently to inhibit the expansion of the sample and therefore, the phase transition. Without the

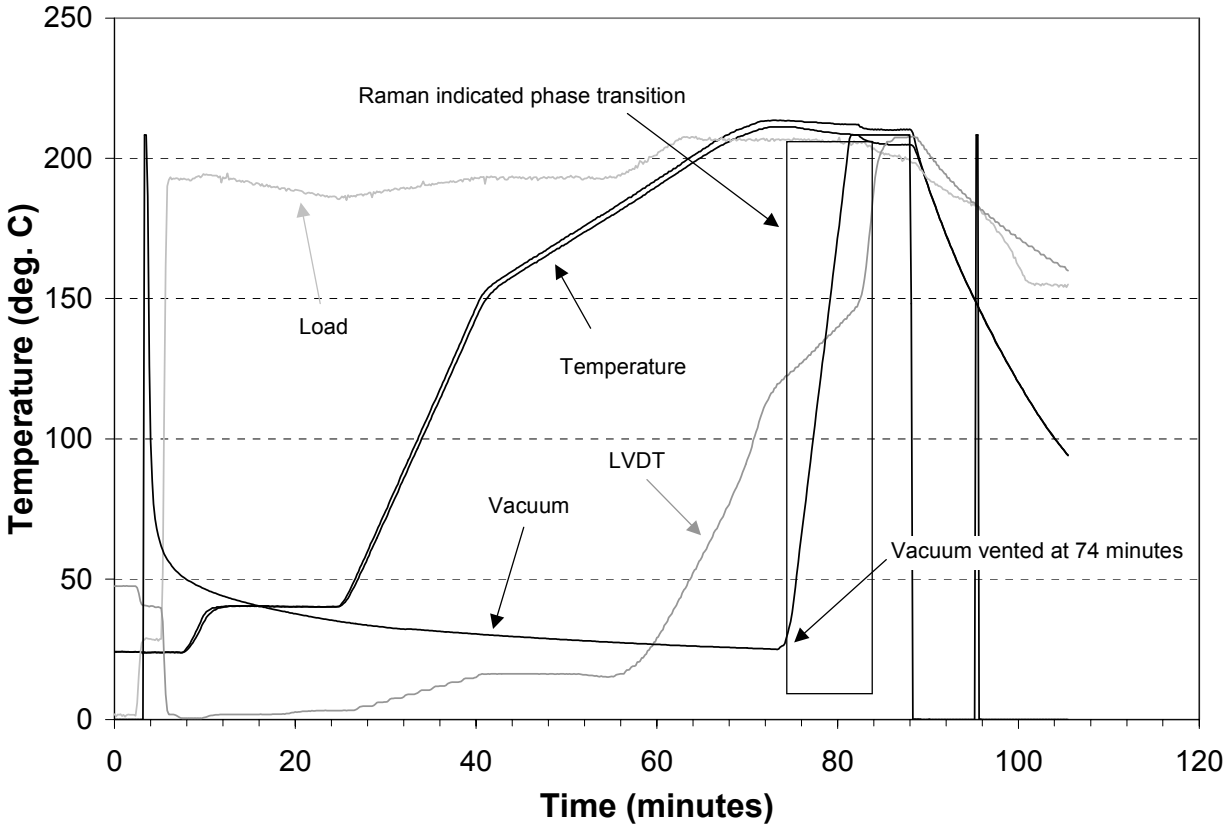

Figure 7. Vacuum effect on phase transition. Upon venting vacuum chamber to atmosphere, the phase transition was induced.

confinement of the window, the pellet would be free to expand at the point of Raman sampling and the phase transition would be detected. The explosives chamber was evacuated and normal heating conducted. At a cell temperature of over 210 °C, at which the phase transition should have normally occurred, no phase transition was observed in the Raman data. After holding the cell at this temperature for some time, the explosive chamber was vented to atmosphere, at time equal to 74 minutes, to investigate if the vacuum was inhibiting the phase transition. This immediately induced the phase transition. The vacuum could have had two possible effects on the phase transition. First, it is possible that, through destabilization of the β phase, the phase transition is induced by decomposition products normally present in thermal decomposition experiments, as discussed by Karpowicz and Brill.[7] Perhaps the presence of any gas is sufficient. Second, the introduction of air around the apparatus could result in greater convective heating of the surface of the sample, which otherwise could remain at a temperature too low for the phase transition to occur. It seems that the first of these two possibilities is more plausible, due to our observation that the surface of the sapphire does reach a sufficiently high temperature for the phase transition to occur and also due to results from an unpublished experiment in which the phase transition was observed immediately upon the introduction of air into an evacuated heating experiment.[13] Due to these findings and the possibility that the vacuum was removing decomposition products, all Raman experiments presented in the remainder of this report were not conducted in vacuum. As a result of this, it was impossible to tell during an experiment if a rapid O-ring failure occurred. This was not of major concern, because the goal of these experiments was not to take the HMX samples to significant decomposition, where high pressure gaseous decomposition products could potentially cause an O-ring to fail, but to investigate the phase transitions. The programmed heating ramp on all subsequent experiments involved heating the cell to 40 °C at 7 K/min, holding for 15 min to allow thermal equilibration, heating to 150 °C at 7 K/min, heating to 205 °C at 2 K/min, holding for 15 min and finally cooling to 50 °C at a rate of 2 K/min. In other hot cell experiments at a final soak temperature of 205 °C, we have not observed O-ring failure at less than one hour holding time. Inspection of O-rings after each subsequent experiment revealed that not one of the O-rings failed, confirming O-ring failure was not of concern.

Temperature Calculation

The recorded temperatures differed considerably from the temperature of the pellet, because the thermocouples were installed in the cell, some distance from the actual pellet. Two internal cell temperatures were recorded by the data acquisition system. Due to the asymmetry of the band heater used on the cell, and the fact that the two thermocouples were located at opposite sides of the cell, the temperature difference was up to 8 °C. In order to correct for the temperature difference between the recorded temperature and the actual pellet temperature, an experiment was conducted in which an additional thermocouple was mechanically bonded to the sapphire window, through which Raman sampling would normally occur, utilizing OMEGATHERM “201” (Omega, Stamford, CT) paste to ensure sufficient thermal conduct. The data from this experiment are shown in Figure 8. It is apparent that the temperatures recorded by the two cell thermocouples are considerably higher than the temperature experienced by the pellet at the site sampled by the Raman probe. The endothermicity of the β-δ phase transition is clearly seen in this figure as a depression in the heating curve measured by the thermocouple in contact with the sapphire window. The β-δ phase transition is an endothermic event and therefore any thermocouple in close contact with the sample will see a depression in the heating ramp during the phase transition. For this reason, a linear extrapolation was performed to compensate for the endothermicity of the phase transition, i.e., reported temperatures do not take the temperature depression of the phase transition into account. To do this would require a separate calibration experiment for each different experiment.

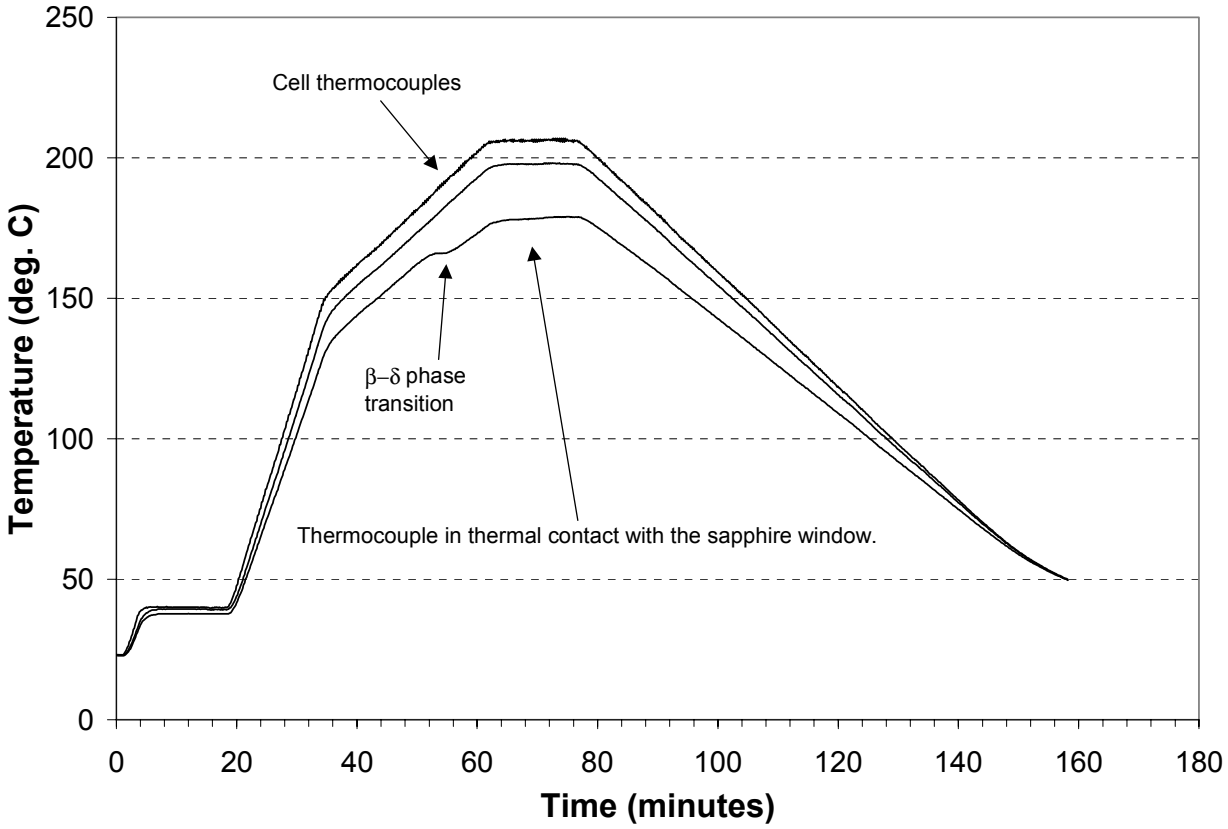

Figure 8. Temperature correction graph. The thermocouple of lower temperature was in contact with the sapphire window and the thermocouples of higher temperature were installed in the cell. The endothermicity of the HMX β-δ phase transition caused the depression in the lower thermocouple measurement.

Typical Experimental Results

Several load-controlled experiments were conducted at various preloads. The results from a typical experiment are shown in Figure 9. In this particular experiment, the sample was preloaded to 14 MPa (2000 psi). The two thermocouple traces of higher temperature indicate the temperature measured during the experiment. The third, lower temperature is that calculated based on the previously mentioned temperature calibration experiment and is a better indicator of the actual pellet temperature. The break in the calculated temperature is due to the difficulty in calculating an accurate value of the final hold temperature because of the endothermicity of the β-δ phase transition as seen in the depression in the measured temperature in Figure 8. Throughout the experiment, the load remained at a relatively constant value, except for two minor excursions associated with the β-δ phase transition during the heating cycle and δ-β/α phase transition during the cooling cycle. The reverse phase transition was not to a pure phase, but rather to a mixture of α- and β-HMX. No attempt was made to quantify the relative ratios of the polymorphs in this mixture. These two phase transitions involve a volume increase (β-δ) and decrease (δ-α/β), and accounted for only a 8% maximum change in the measured load in this load-controlled experiment, whereas in the displacement-controlled variation of this experiment, load changes of over 200% are not uncommon. This smaller change is due to the fact that the compressibility of the pneumatic cylinder can only minimize the effects of expansion and contraction of the pellet, but cannot completely eliminate them. The two boxes in Figure 9 represent the detection of the phase transition by Raman

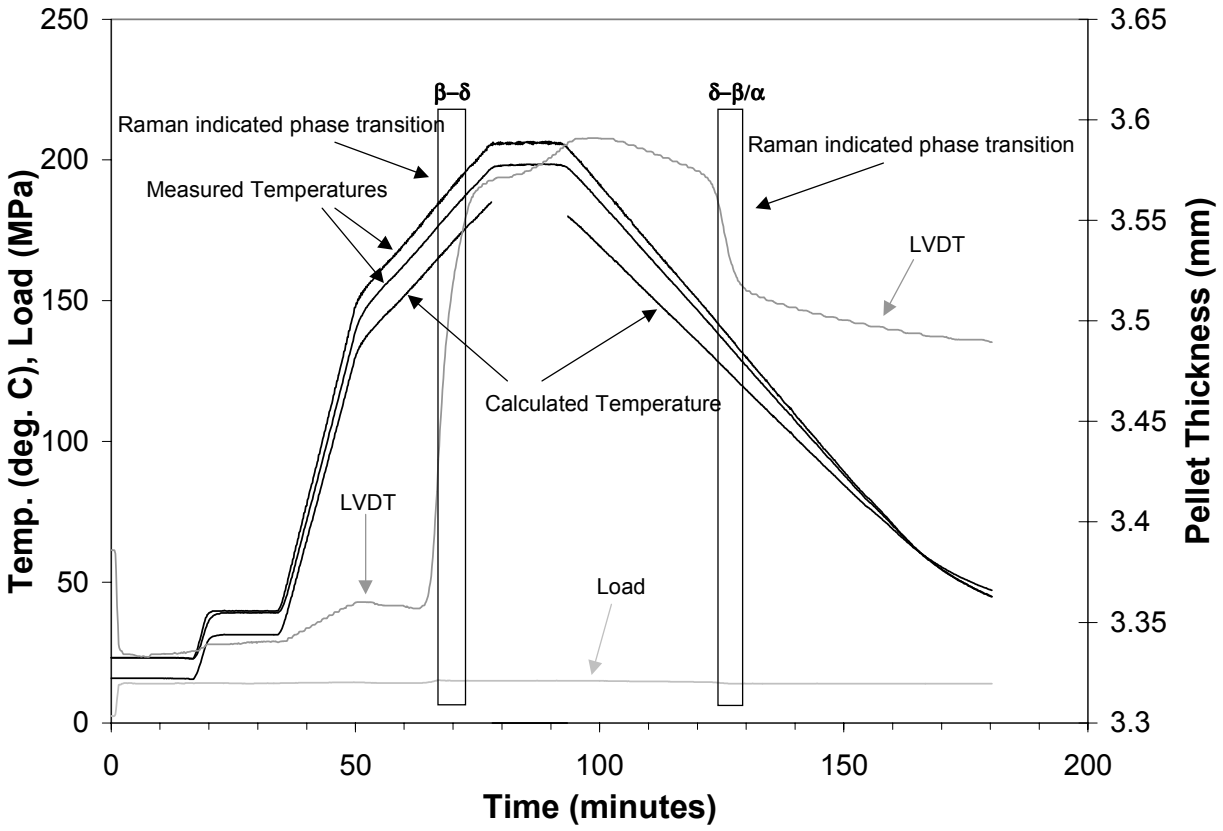

Figure 9. Temperature and load cell response for typical load-controlled experiment. Sample preload was 14 MPa. The boxes indicate phase transitions as detected by Raman spectroscopy.

spectroscopy, with the first box indicating the β-δ phase transition and the second box indicating the δ-β/α phase transition. The volume increase associated with the β-δ phase transition and the volume decrease associated with the δ-β/α phase transition are clearly seen in the sample length data. The fact that the sample length data and the Raman data overlap in this experiment is not representative of all experiments. There were cases in which the phase transition detected by the Raman data preceded the sample length data and vice versa. In initial experiments, there were situations where the LVDT detected the phase transition and it was not seen in the Raman data. This is due to the fact that sample length is a bulk measurement and Raman spectroscopy involves a surface point measurement. Small differences in the local area of Raman sampling can greatly affect the measurement. We have observed that in HMX samples, different areas having apparently similar conditions can undergo the phase transition at different times. This can be due to different particle sizes or perhaps different local stress states, or differing thermal contact. If the point of sampling happens to be in an area that is not representative of the bulk material, anomalous data can result.

The Raman spectroscopic data from this experiment, for both the forward (β-δ) and reverse (δ-β/α) phase transitions, are shown in Figure 10. The β-δ phase transition is indicated by the disappearance of the β peaks at 356 and 428 cm^{-1} and the appearance of the δ peak at 385 cm^{-1}. In addition, the β peaks at 829 and 945 cm^{-1} disappear and are replaced by δ peaks at 841 and 932 cm^{-1}, respectively. The persistence of the peak at 412 cm^{-1} through the phase transition was consistent in all of the experiments mentioned in the remainder of this report. This result is inconsistent with results of Goetz and Brill.[5] The significance of this is not known. The β-δ phase transition occurred over the calculated temperature

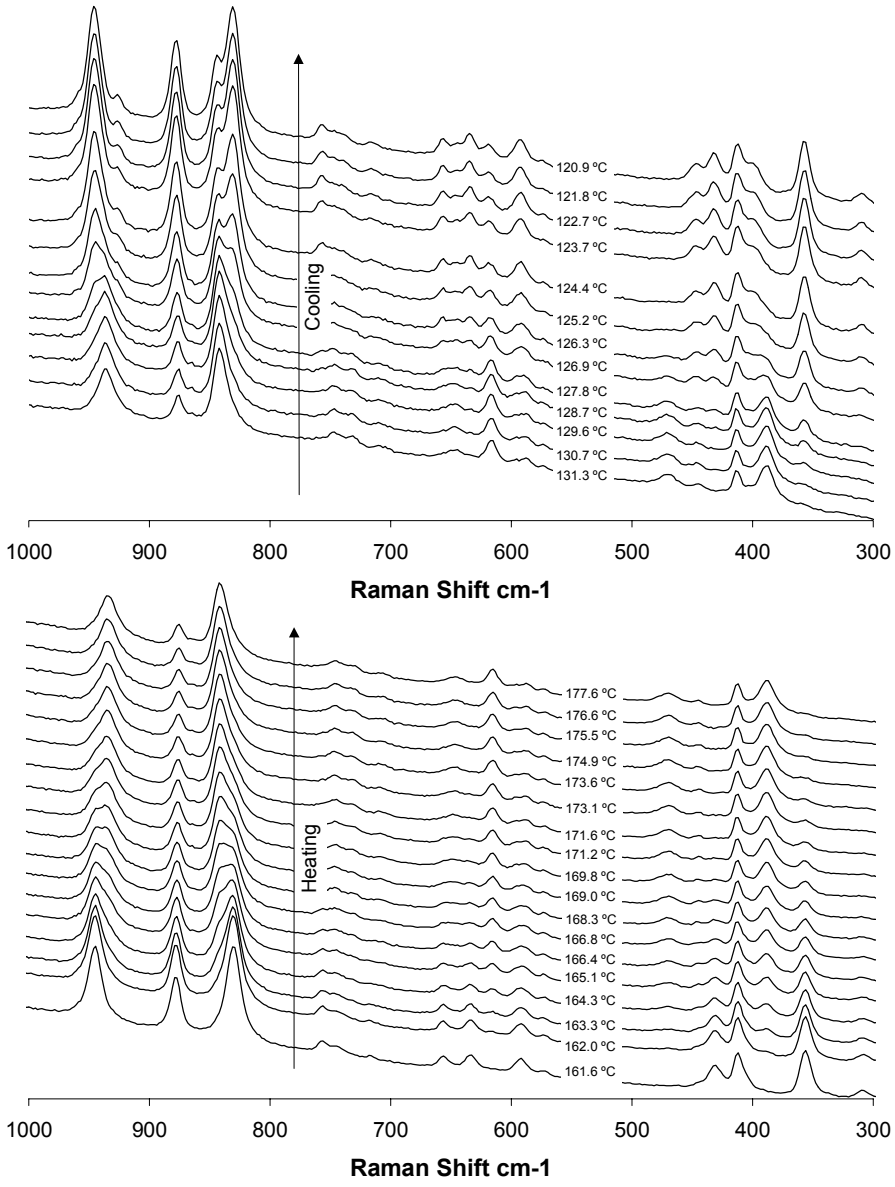

Figure 10. Successive Raman spectra of HMX phase transition during heating (lower graph, β→δ) and cooling (upper graph, δ→α/β). Sample preload was 14 MPa.

range of 162 to 178 °C. During this observation of the phase transition in the Raman data, a volume increase of the pellet was observed in the pellet length data. The total increase in length during the phase transition, as indicated from the pellet length data, was 0.21 mm or 6.25 %. This can be assumed to also be the increase in volume, because the pellet is heavily confined from the sides and only allowed to expand in length. The increase in pellet length during the phase transition, indicated by the Raman data, is somewhat less, due to the consistent result that the Raman data did not capture the entire bulk phase transition, which was captured by the pellet length data, but only that portion which occurred at the site of Raman sampling. In addition to the length change, there was a slight increase in the load data from 14.31 to 14.89 MPa (2076 to 2173 psi) or 4.1 %. This period of change in load represents the largest load change during any given load-controlled experiment and is due to the inability of the pneumatic cylinder to completely absorb load changes. This is very small compared to the 200% load changes seen in displacement-controlled experiments. The reverse, δ-β/α phase transition was indicated by the disappearance of the δ peaks at 387, and 936 cm^{-1} and the appearance of the β peaks at 356, and 430 cm^{-1} and α peaks at 398, 445, 829, 925 and 945 cm^{-1}. It is important to note that because the forward and reverse phase transitions occurred at different temperatures, peaks for the same vibrational transition have different values, with higher temperatures shifting the peaks towards lower values of Raman shift. An interesting effect was seen in each experiment in which, a few minutes before each reverse phase transition, the intensity of the entire spectrum increased, the phase transition began to occur and the intensity then decreased. It is possible that this effect was due to the exothermicity of the reverse phase transitions and that some heating of the sample caused a more intense broadband emission. This effect was seen in the initial heating of the

sample as each spectrum had a higher overall intensity than the one previous. The complimentary effect was seen in the β-δ phase transition, in which heating of the sample caused the overall emission to increase, but just prior to, and during the phase transition, the overall emission decreased a slight amount due to the cooling caused by the endothermicity of the β-δ phase transition.

Load-Temperature Dependence

Due to the different densities of the different phases of HMX, the temperatures of phase transitions are pressure dependent.[6] Load-controlled experiments were conducted at various loads to explore this dependence in our experimental configuration. The phase transitions were detected using Raman spectroscopy and also by using the pellet length measurement to observe the volume changes associated with the phase transitions. Experiments were conducted at constant loads of 2.8 to 28 MPa (407 to 4070 psi). Three comparisons were made with the load: calculated temperature at the onset of the phase transition, calculated temperature at the completion of the phase transition and the time necessary for the completion of the phase transition. For the reverse phase transition, all possible phase transitions were treated the same, regardless of whether the reverse phase transition was δ-α, δ-β, or δ to a mixture. All possible mixtures were observed, except α/δ, and are listed in Table 1. At the lowest load of 2.8 MPa (407 psi), the onset of the reverse phase transition was observed in the Raman spectrum, but not in the pellet length data and the completion of the reverse phase transition was not observed in the Raman data, nor the pellet length data.

The data for the temperature of both the onset and completion of the forward phase transition, as detected by both Raman spectroscopy and pellet length, versus load, with linear regressions, are shown in Figure 11. The phase transition was always β-δ. All samples experienced the same heating ramp. At the onset of the phase transition, the sample was always β-HMX and at the completion, the sample was always δ-HMX. A strong correlation between load and temperature of phase transition was not discovered in any of the forward phase transition data. Some trends in the data are apparent, however. The temperature of the onset of the phase transition as detected by Raman spectroscopy versus load shows significant scatter and has a correlation coefficient (R^2) of only 0.46. Although the correlation coefficient is very low, the trend is that higher preloads cause the phase transition to begin at lower temperatures. This result is inconsistent with the trend in the temperature of onset of phase transition as detected by pellet length, of higher preloads causing the phase transition to begin at higher temperatures. It is also inconsistent with the results of Landers and Brill.[6] Although the correlation is low, the temperature of the onset of the β-δ phase transition, as detected by pellet length measurements data show the expected trend of higher loads causing the phase transition to occur at higher temperatures. Within the temperature of completion of phase transition data, a trend is visible in both the Raman and pellet length data. The trend is that higher loads cause the phase transition to complete at higher temperatures, but the correlation coefficients for these data are also very low. Possible reasons for the unexpected results of the temperature of onset of phase transition as detected by Raman spectroscopy and also for the low correlation in the other data will be discussed in more detail in the last paragraph of this section, after discussion of the reverse phase transitions.

Table 2. HMX phases detected upon cooling for various loads.

Load (MPa)	Load (psi)	HMX phase
2.8	407	β / δ
7.0	1020	β
7.0	1020	β
14.0	2040	α / β
21.0	3060	β
28.0	4070	α

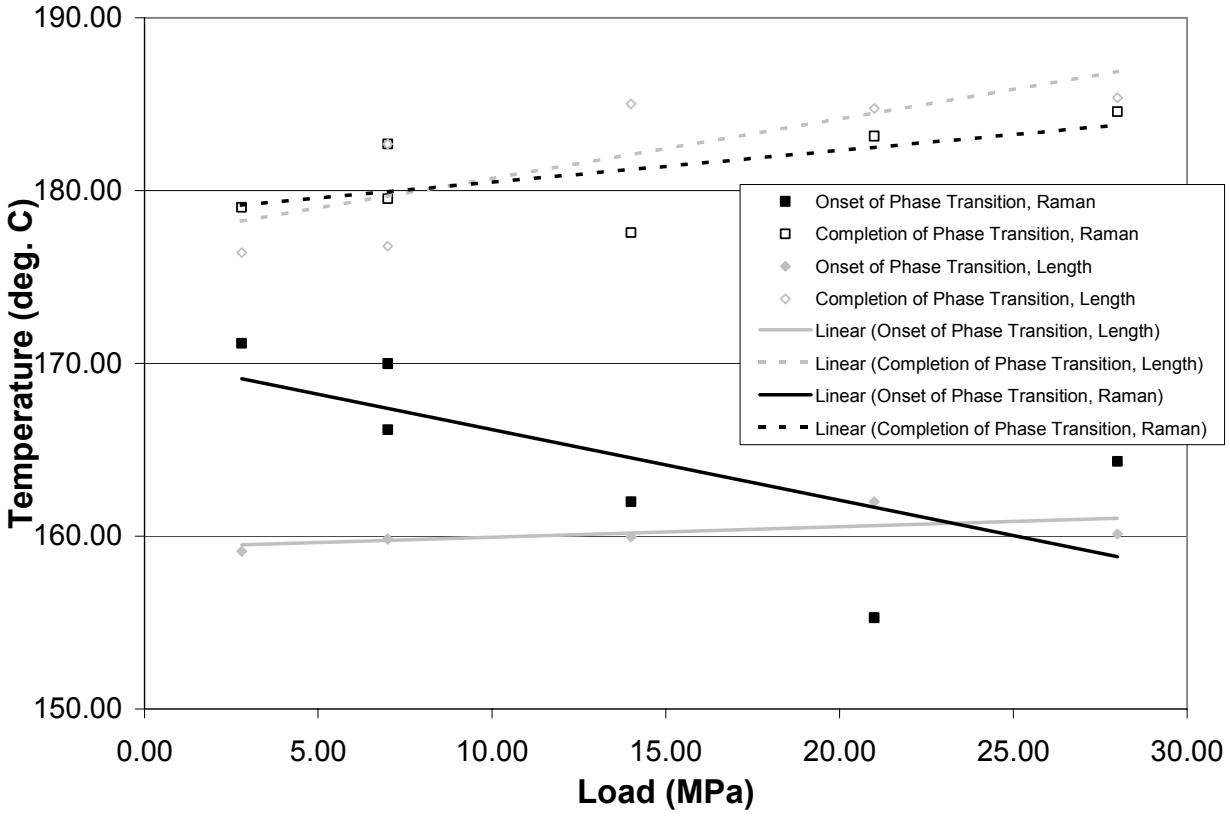

Figure 11. Temperature of forward phase transition versus load as detected by Raman spectroscopy and pellet length measurements.

The data for the temperature of both the onset and completion of the reverse phase transition, as detected by both Raman spectroscopy and pellet length, versus load, with linear regressions, are shown in Figure 12. No distinction between what phase, or mixture of phases, was present at the completion of the experiment was made. In these data, correlations between temperature of phase transition and load were found. All samples experienced the same cooling rate of 2 K/min. At the onset of each reverse phase transition, HMX at the point of Raman sampling was always in the δ phase as a result of heating. Although the starting material was always δ-HMX, α, β, and mixtures of α/β and β/δ were all observed during the reverse phase transition. In postmortem studies of HMX samples, not necessarily from this group of experiments, we have observed several different phases on the same HMX sample. This is important to note because it demonstrates that the point of sampling is not necessarily representative of the bulk material and also that samples in our experimental apparatus experience different thermal and pressure fields across the sample. Insufficient data were obtained to develop pressure regimes for the existence of the different phases, but as shown in Table 1, it is of note that δ-HMX (in a mixture of both β- and δ-HMX) was only observed to persist at the lowest load of 2.8 MPa (407 psi). At higher loads, δ-HMX was not observed, but α-, β- and mixtures of α- and β-HMX were, with no immediately apparent trend. Both Raman spectroscopic data and sample length data show the general trend that higher loads drove the reverse phase transition to occur earlier, i.e., at a higher cooling temperature. This result is consistent with the fact that the density order β-HMX > α-HMX > δ-HMX exists and thus higher pressures would tend to cause δ-HMX to transform to α- and β-HMX at higher loads.[3]

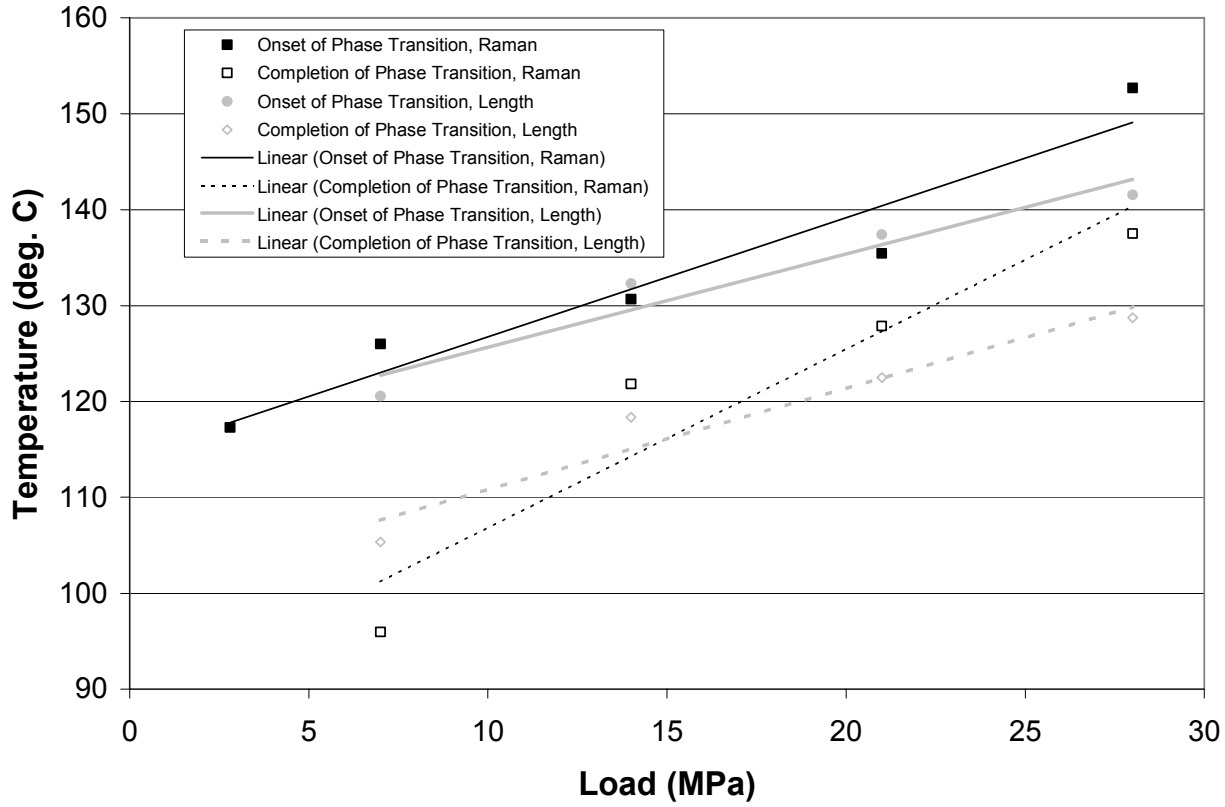

Figure 12. Temperature of reverse phase transition versus load as detected by Raman spectroscopy and pellet length measurements.

The data for time necessary to complete the phase transition, for both the forward and reverse phase transitions, are shown in Figure 13. For the forward, β-δ phase transition, increasing loads tended to cause the phase transition to occur over more time. This is in agreement with the reasoning that increasing the load retards the phase transition, causing HMX to remain in the denser β phase. Although the correlation is not strong, the trend is readily visible from the data. The complimentary trend is present in the reverse phase transition data, in which increasing loads drove the phase transition to occur over less time. The correlation here is very weak, but the trend can be seen in the data. No attempt to perform a linear regression on the Raman spectroscopic data was made, because the high degree of scatter in the data makes such a measurement meaningless. Despite the scatter, the trend is visible that increasing loads drove the phase transition to occur in less time. Again, the reasoning that higher loads cause HMX to transform to the denser β phase applies.

The inability to observe a strong correlation in the temperature of the β-δ, forward phase transition data may be due to one or a combination of factors, but fundamentally may be due to the fact that the pressure, or temperature at the site of sampling was not what it appeared to be. This, in combination with the potentially stochastic nature of the phase transition, could explain the significant scatter in our data. The fact that the results for the temperature of the onset of phase transition as detected by Raman spectroscopy show significant scatter and do not agree with published data suggests that the lack of a correlation may be due to experimental variables, kinetics, damage of material, or some other effect. It may be that an insufficient range of loads was explored, or that insufficient data at this load range were collected. One should be careful to say that a correlation does not exist based on these data,

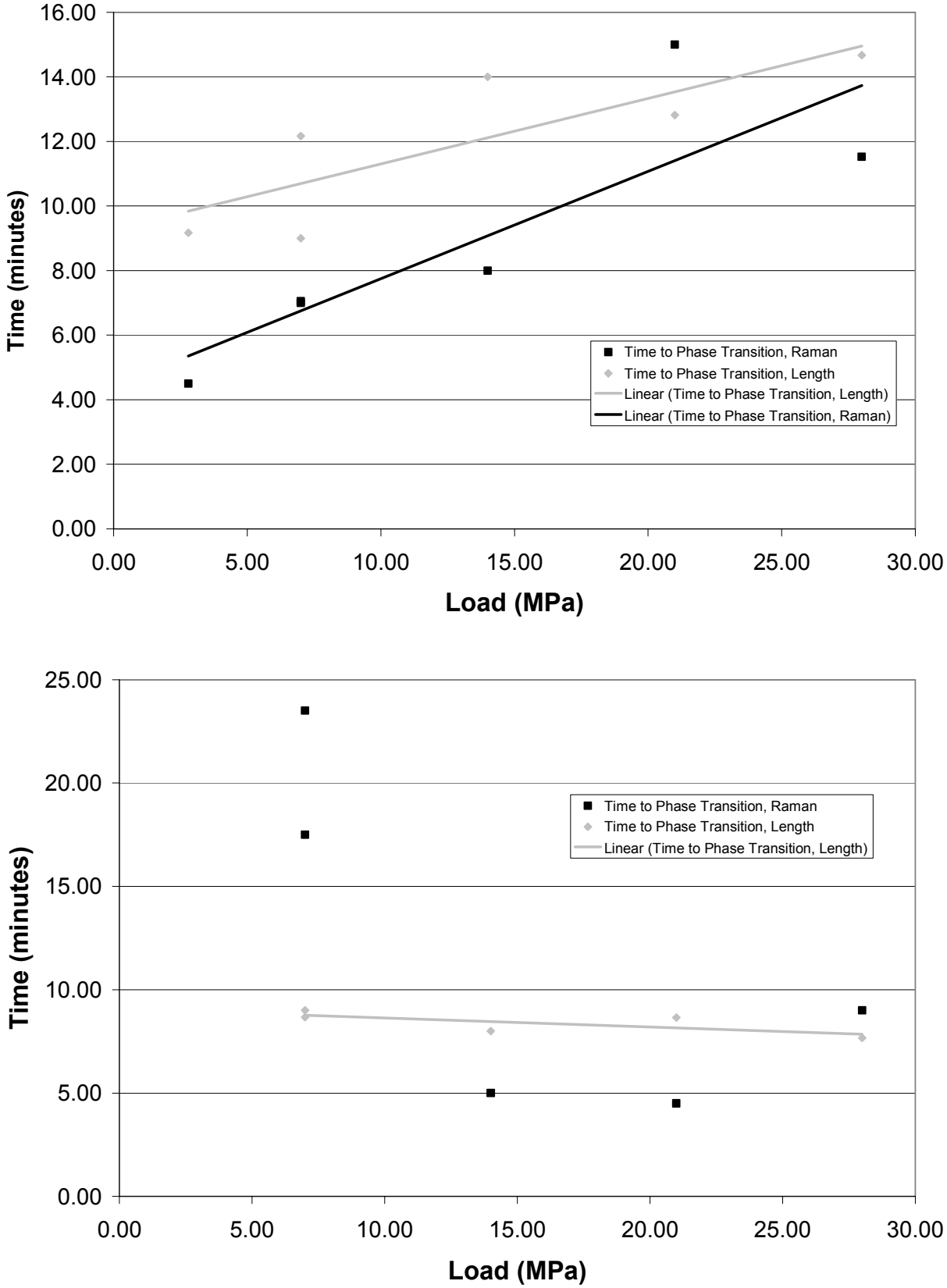

Figure 13. Time necessary to complete the phase transition for both the forward (top, β-δ) and reverse (bottom, δ- α, β or a mixture) phase transitions.

because it has been seen in other experiments, but only that it was not detected using our experimental apparatus. One possibility is that in each different experiment, different temperatures existed at the sampling site. This may have been due to different thermal contact from different loads, inconsistent thermal gradients, or inhomogeneities within the sample. The fact that the temperature of reverse phase transitions versus load presented good correlations and the forward phase transition did not, may suggest that some change during the experiment occurred that improved consistency. One possibility is that the cell had a leak that was present during the initial heating cycle, but sealed with decomposition products as the experiment continued. This sealing could lead to the internal pressure of the cell reaching the gas pressure that was indicated by mechanical loading during the cooling cycle. If the gas pressure of the cell did not match the load as measured during the experiment, scattering of the data could have resulted. Along these same lines, it is possible that in the heating cycle, the pellet sees only a mechanical load because there are insufficient gaseous decomposition products to cause the load cell measurement to represent the gas pressure within the cell. In the cooling cycle, sufficient gaseous decomposition products have been produced to exceed the mechanical load on the pellet causing the load cell measurement to more accurately represent the gas pressure within the cell. This could explain the lack of load versus temperature of phase transition correlation during the heating cycle that is present during the cooling cycle. Another possibility is that inconsistent thermal gradients existed across the pellet during the heating cycle that were not present during the cooling cycle. This could be due to voids being crushed out during the expansion thus creating a more uniform thermally conductive material. It is also possible that the cooling cycle simply resulted in inherently more uniform thermal gradients across the hot cell than the heating cycle did. It is important to note that Raman spectroscopy provides only a surface measurement and therefore, is only sampling a small fraction of the bulk sample. The phase transition, however, is a bulk phenomenon and this mismatch of detection technique with scale of phenomenon may be a significant source of error. The inability to observe a load-temperature dependence in the β-δ phase transition is most likely due to the mechanical load not representing the pressure within the cell. The fact that the reverse phase transition did show a dependence supports this argument, because the presence of sufficient gaseous decomposition products would cause the load cell to represent the gas pressure within the cell.

SUMMARY AND CONCLUSIONS

We have demonstrated the ability to monitor the HMX β-δ phase transition in the hot cell apparatus with Raman spectroscopy. Both postmortem and real-time Raman spectroscopic measurements demonstrate that regions within the same small sample can exhibit differing phase transition characteristics, despite seemingly identical environmental conditions of pressure and temperature. The effect of regions of HMX undergoing the β-δ phase transition and inhibiting the phase transitions in adjacent areas has been demonstrated. Shape of components may affect EM confinement in a cookoff scenario, resulting in areas of low confinement in which the phase transition could occur to a greater extent, compared with areas of high confinement, in which the phase transition would be inhibited. We have investigated the load-temperature dependence of the phase transition in the hot cell apparatus. The temperature of the onset of the β-δ phase transition did not demonstrate a strong correlation with load. However, the temperature of the β-δ phase transition as indicated by pellet length showed a trend of higher loads causing the phase transition to occur at higher temperatures. This was especially true when the temperature at the end of the phase transition was used as the indicator. The trend was less apparent in the Raman data. This is believed to be due to the load indicated by the load cell not representing the gas pressure within the cell until sufficient gaseous decomposition products had been produced. It could also potentially be due to other problems in our experimental apparatus, such as a leak in the cell or inconsistent thermal gradients, or to the potentially random nature of the destabilization of the β phase, a

necessary step for the phase transition to occur. The δ-α, δ-β and δ-α/β phase transitions, which occur during the cooling of the sample, all showed a correlation between load and temperature of phase transition. Higher loads drove the phase transition to occur earlier, at higher cooling temperatures. The time necessary for the completion of the β-δ phase transition increased for increasing loads. The time necessary for completion of the reverse phase transitions decreased with increasing loads. Finally, the analysis with Raman spectroscopy demonstrates that the expansion seen in the load cell and LVDT extensometer data is in fact due to the phase transitions and not to anomalous expansions and contractions of the material. Raman spectroscopy is an excellent technique to distinguish the phases of HMX. However, it is important to recognize that it is a surface technique and samples only a small area. The HMX phase transitions are bulk phenomena and must be treated as such.

REFERENCES

1) Tappan, A. S., Renlund, A. M., Gieske, J.H. and Miller, J.C., "Raman Spectroscopic and Ultrasonic Measurements to Monitor the HMX β-δ Phase Transition," Proceedings of the 1999 JANNAF Propulsion Systems Hazards Subcommittee Meeting, Cocoa Beach FL (1999).
2) Tappan, A. S., Renlund, A. M., Gieske, J.H. and Miller, J.C., "Real-Time Raman Spectroscopic and Ultrasonic Measurements to Monitor the HMX β-δ Phase Transition and Physical Changes in Thermally Damaged Energetic Materials," Proceedings of the 2000 JANNAF Propulsion Systems Hazards Subcommittee Meeting, Monterey, CA (2000).
3) Cady, H. H., Larson, A. C., Cromer, D. T., "The Crystal Structure of α-HMX and a Refinement of the Structure of β-HMX," *Acta Crystallografica*, **16**, 617-623, (1963).
4) Cady, H. H. and Smith, L. C., "Studies on the Polymorphs of HMX," LAMS-2652, Los Alamos Scientific Laboratory, (1962).
5) Goetz, F. and Brill, T. B., "Laser Raman Spectra of α-, β-, γ-, and δ-Octahydro-1,3,5,7-tetranitro-1,3,5,7-tetrazocine and Their Temperature Dependence," *The Journal of Physical Chemistry*, **83**, 340-346, (1979).
6) Landers, A. G. and Brill, T. B., "Pressure-Temperature Dependence of the β-δ Polymorph Interconversion in Octahydro-1,3,5,7-tetranitro-1,3,5,7-tetrazocine," *The Journal of Physical Chemistry*, **84**, 3573-3577, (1980).
7) Karpowicz, R. J. and Brill, T. B., "The β→δ Transformation of HMX: Its Thermal Analysis and Relationship to Propellants," *AIAA Journal*, **20**, 1586-1591, (1982).
8) Teetsov, A. S. and McCrone, W. C., "The Microscopial Study of Polymorph Stability Diagrams," *Microsc. Cryst. Front*, **15**, 13-29 (1965).
9) Renlund, A. M., Miller, J. C., Hobbs, M. L., Baer, T. A. and Baer, M. R., "Experimental and Analytical Characterization of Thermally Degraded Energetic Materials," Proceedings of the 1995 JANNAF Propulsion Systems Hazards Subcommittee Meeting, Huntsville, AL (1995).
10) Hobbs, M. L., Schmitt, R. G. and Renlund, A. M., "Analysis of Thermally-Degrading, Confined HMX," Proceedings of the 1996 JANNAF Propulsion Systems Hazards Subcommittee, Monterey, CA (1996).
11) Iqbal, S. Bulusu, S. and Autera, J. R., "Vibrational spectra of β-cyclotetramethylene tetranitramine and some of its isotopic isomers," *Journal of Chemical Physics*, **60**, 221-230, (1974).
12) Herrmann, M., Engel, W., and Eisenreich, N., "Thermal analysis of the phases of HMX using X-ray diffraction," *Zeitschrift für Kristallographie*, **204**, 121-128, (1993).
13) Wayne Trott, Sandia National Laboratories, private communication.

APPENDIX

Abstracts of references 1 and 2 at which work based on this LDRD was presented.

Reference 1:

Raman Spectroscopic and Ultrasonic Measurements to Monitor the HMX β-δ Phase Transition

A.S. Tappan, A.M. Renlund, J.H. Gieske and J.C. Miller

Sandia National Laboratories*, Albuquerque, NM

ABSTRACT

The HMX β-δ solid-solid phase transition, which occurs as HMX is heated near 170°C, is clearly linked to increased reactivity and sensitivity to initiation. Thermally damaged energetic materials (EMs) containing HMX therefore may present a safety concern. Information about the phase transition is vital to a predictive safety model for HMX and HMX-containing EMs. We report work in progress on monitoring the phase transition with real-time Raman spectroscopy and ultrasonic measurements aimed towards a better understanding of physical properties through the phase transition. HMX samples were confined with minimal free volume in a cell with constant volume. The cell was heated at a controlled rate and real-time Raman spectroscopic or ultrasonic measurements were performed. Raman spectroscopy provides a clear distinction between the two phases because the vibrational transitions of the molecule change with conformational changes associated with the phase transition. Ultrasonic time-of-flight measurements provide an additional method of distinguishing the two phases because the sound speed through the material changes with the phase transition. Ultrasonic attenuation measurements also provide information about microstructural changes such as increased porosity due to evolution of gaseous decomposition products.

Reference 2:

Real-Time Raman Spectroscopic and Ultrasonic Measurements to Monitor the HMX β-δ Phase Transition and Physical Changes in Thermally Damaged Energetic Materials

A.S. Tappan, A.M. Renlund, J.H. Gieske and J.C. Miller

Sandia National Laboratories*, Albuquerque, NM

ABSTRACT

The HMX β-δ solid-solid phase transition, which occurs as HMX is heated near 170°C, is linked to increased reactivity and sensitivity to initiation. Thermally damaged energetic materials (EMs) containing HMX therefore may present a safety concern. Information about the phase transition is vital to predictive safety models for HMX and HMX-containing EMs. We report work on monitoring the phase transition and physical changes with real-time Raman spectroscopy and ultrasonic measurements, aimed towards a better understanding of physical property changes through the phase transition and during decomposition. EM samples were confined with minimal free volume in a cell in either a displacement-controlled or load-controlled arrangement. The cell was heated at a controlled rate and real-time Raman spectroscopic or ultrasonic measurements were performed. Raman spectroscopy provides a clear distinction between β- and δ-HMX, because the vibrational transitions of the molecule change with conformational changes associated with the phase transition. Temperature-pressure dependence data for the HMX phase transition are reported, in addition to data for the reverse phase transition as the sample was cooled. Ultrasonic time-of-flight measurements provide an additional method of distinguishing the two phases because the sound speed through the material changes with the phase transition. Ultrasonic velocity and attenuation measurements also provide information about microstructural changes such as increased porosity due to evolution of gaseous decomposition products. Real-time elastic moduli data from ultrasonic experiments are reported for HMX. In addition, we report results of ultrasonic experiments for the RDX-containing EM, PBXN-109.

DISTRIBUTION

3 Lawrence Livermore National Laboratory
P.O. Box 808
Livermore, CA 94551-0808
ATTN:
MS L-282 Jerry W. Forbes
MS L-282 Jon L. Maienschein
MS L-282 Joseph M. Zaug

6 Los Alamos National Laboratory
P.O. Box 1663
Los Alamos, NM 87545
ATTN:
MS C920 Blaine W. Asay, DX-2
MS C920 Michele E Decroix, DX-2
MS C920 Steven F. Son, DX-2
MS G755 Peter Dickson, DX-2
MS J567 Bryan F. Henson, C-PCS
MS J585 Laura B. Smilowitz, C-PCS

36 Internal:
MS 0188 LDRD Office, Donna L. Chavez, 01030
MS 0521 Thomas J. Cutchen, 02501
MS 0615 John H. Gieske, 09122
MS 0834 Arthur C. Ratzel, 09112
MS 0834 Wayne M. Trott, 09112
MS 0836 William W. Erikson, 09116
MS 0836 Eugene S. Hertel, Jr., 09116
MS 0836 Leanna M. G. Minier, 09116
MS 0836 Robert G. Schmitt, 09116
MS 0953 James K. Rice, 02500
MS 1452 Christopher A. Gresham, 02552
MS 1452 John A. Merson, 02552
MS 1453 Gregory L. Scharrer, 02553
MS 1454 Anita M. Renlund, 02554 (5)
MS 1454 Lloyd L. Bonzon, 02554
MS 1454 Michael J. Kaneshige, 02554
MS 1454 Jill C. Miller, 02554
MS 1454 Alexander S. Tappan, 02554 (10)
MS 9052 Richard Behrens, Jr., 08361

MS 9018 Central Technical Files, 8945-1
MS 0899 Technical Library, 9616 (2)
MS 0612 Review & Approval Desk, 9612
For DOE / OSTI

Intentionally Left Blank